

## Case Report | Pediatric Imaging

<http://dx.doi.org/10.3348/kjr.2013.14.2.361>

pISSN 1229-6929 · eISSN 2005-8330

Korean J Radiol 2013;14(2):361-365

Korean Journal of Radiology



# Cellular Mesoblastic Nephroma with Liver Metastasis in a Neonate: Prenatal and Postnatal Diffusion-Weighted MR Imaging

Seok-min Ko, MD<sup>1</sup>, Myung-Joon Kim, MD<sup>1</sup>, Young-Jae Im, MD<sup>2</sup>, Kook-In Park, MD<sup>3</sup>, Mi-Jung Lee, MD<sup>1</sup>

Departments of <sup>1</sup>Radiology and Research Institute of Radiological Science, <sup>2</sup>Pediatric Urology and <sup>3</sup>Pediatrics, Severance Children's Hospital, Yonsei University College of Medicine, Seoul 120-752, Korea

Congenital mesoblastic nephroma (CMN) is the most common renal tumor in the first year of life. Here, we present unique findings of cellular variant CMN seen on prenatal and postnatal MRI with diffusion-weighted imaging (DWI). The mass was well-visualized on prenatal MR DWI with diffusion restriction in the solid portions. After excision of the mass, follow-up whole body MRI with DWI helped identify local tumor recurrence with suspicious liver metastasis. This hepatic lesion also showed diffusion restriction.

**Index terms:** Congenital mesoblastic nephroma; MRI; Diffusion-weighted imaging

## INTRODUCTION

Congenital mesoblastic nephroma (CMN) was first described in 1967 by Bolande et al. (1) as a leiomyoma-like tumor of the kidney. It is the most commonly occurring renal tumor found in infants less than three months old, and known to have a favorable outcome after complete surgical excision (2). Joshi et al. (3) summarized the main pathological variants of CMN as the classic variant and cellular variant. According to previous studies, the cellular variant demonstrates more local recurrence and distant metastasis with the reported local recurrence rate of 10-17% (4, 5). The cellular variant can be accompanied by

intratumoral hemorrhage with a large cystic or necrotic component (5). Invasion of the perirenal fat and adjacent organs, as well as evidence of local recurrence, are also commonly seen in the cellular variant (3).

There have been reports about CMN findings on ultrasonography (US), computed tomography (CT) and magnetic resonance imaging (MRI) (4-7). However, there have been no published reports about diffusion-weighted imaging (DWI) findings of CMN. DWI can be helpful to differentiate renal tumors, even though there are some debates (8-10). Here, we report a case of CMN with prenatal and postnatal MR imaging, including DWI.

## CASE REPORT

A 30-year-old woman pregnant with a fetus at 30 weeks gestational age was referred to the obstetrics department of our hospitals, due to an increasing fetal abdominal mass. The fetal mass was first detected at 26 weeks gestation on a routine antenatal US at a local clinic. The mother had no contributing medical or surgical history to explain the mass growth. Another fetal US was performed in the emergency room with a 1-5 MHz curved array transducer (IU22, Philips Medical Systems, Best, The Netherlands). This US revealed a

Received June 29 2012; accepted after revision September 19, 2012.

**Corresponding author:** Mi-Jung Lee, MD, Department of Radiology and Research Institute of Radiological Science, Severance Children's Hospital, Yonsei University College of Medicine, 50 Yonsei-ro, Seodaemun-gu, Seoul 120-752, Korea.

• Tel: (822) 2228-7400 • Fax: (822) 393-3035

• E-mail: [mjl1213@yuhs.ac](mailto:mjl1213@yuhs.ac)

This is an Open Access article distributed under the terms of the Creative Commons Attribution Non-Commercial License (<http://creativecommons.org/licenses/by-nc/3.0>) which permits unrestricted non-commercial use, distribution, and reproduction in any medium, provided the original work is properly cited.

huge left abdominal mass that was composed of both solid and cystic areas, and Doppler US also showed increased vascularity. Fetal cardiomegaly and polyhydramnios were also detected.

A fetal MRI was obtained on the same day using a 1.5T MR scanner (InteraAchieva, Philips Medical Systems, Best, The Netherlands). Single-shot turbo spin-echo sequences (in the axial, coronal, and sagittal planes), coronal T1-weighted images with spectral presaturation inversion recovery, and axial DWI using four b-values (0, 50, 400, 800  $\text{smm}^{-2}$ ) were obtained. The MRI showed a huge soft tissue mass (about 8 x 9 x 10 cm) in the left fetal retroperitoneum (Fig. 1A-C). This mass not only displaced the abdominal aorta, but also moved the bowel loops to the right. The right kidney was seen in the right renal fossa, but the left kidney was not visualized. Solid portions in the mass had multiple cystic spaces. The solid portions were of low signal intensity on the T1-weighted images and of intermediate signal

intensity on the T2-weighted images. On DWI, diffusion restriction was observed in the solid portions of the mass with apparent diffusion coefficient (ADC) value of  $1.02 \times 10^{-3} \text{ mm}^2/\text{sec}$ . No hemorrhage or necrosis was observed.

An emergency caesarian section to deliver the female infant was performed the next day due to signs of preterm labor and fetal distress. Immediately after birth, an abdominal radiograph showed a large soft tissue mass occupying the neonate's left abdomen. An abdominal US also showed a huge mass with solid and cystic portions in the left retroperitoneum, as previously seen on the fetal MRI (Fig. 1D). Additionally, the mass compressed the aorta to the right without evidence of encasement. The right kidney showed diffusely increased parenchymal echogenicity with renal pelvic dilatation.

Five days after birth, the neonate underwent radical excision of the tumor in the left retroperitoneum. The surgeon reported that the mass originated from the left

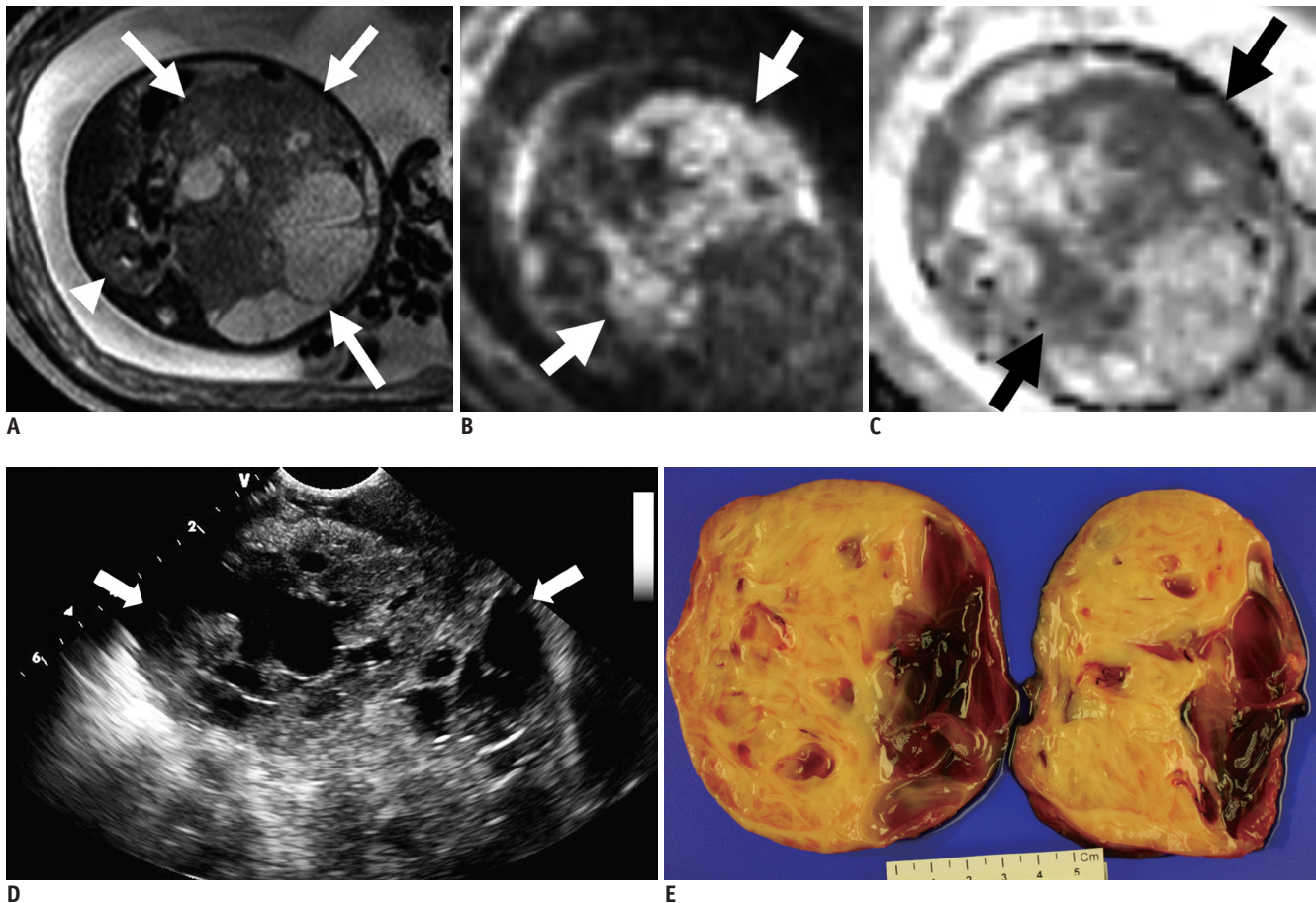


**Fig. 1. Cellular mesoblastic nephroma in a female neonate.**

**A-C.** Fetal MRI shows huge mass (arrows) occupying left retroperitoneum. Solid portions show intermediate signal intensity on axial T2-weighted image (**A**) and right kidney (arrowhead) is visible. Solid portion of mass shows true diffusion restriction on diffusion-weighted imaging (**B**, white arrows) and on apparent diffusion coefficient map (**C**, black arrows). **D.** Postnatal, preoperative ultrasonography shows huge solid and cystic mass (arrows) in left abdomen. **E.** Gross pathology of resected mass is composed of solid and cystic portions.

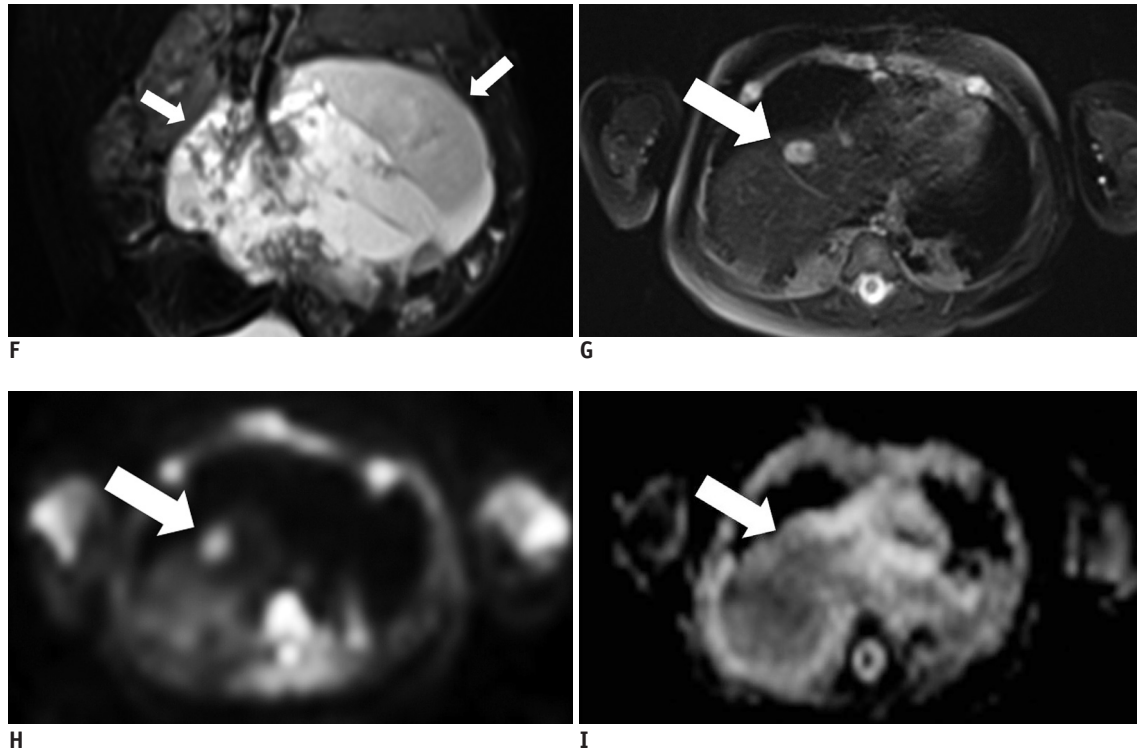


**Fig. 1. Cellular mesoblastic nephroma in a female neonate.**

**F-I.** Whole body MRI during follow-up shows huge cystic recurrent mass (arrows) in left retroperitoneum on T2-weighted image (**F**) with liver dome mass (arrow), appearing as high signal on T2-weighted image (**G**) and diffusion restriction on diffusion-weighted imaging (**H**) and apparent diffusion coefficient map (**I**).

kidney that crossed the midline and was composed of solid and cystic lesions. The upper and posterior aspect of the mass was severely adhered to the peritoneum, without bowel adhesion.

On pathologic review, the mass was grossly found to be composed of solid and cystic portions and confirmed as originating from the left kidney (Fig. 1E). On microscopic examination, there were uniform fascicles of spindle cells with increased cellularity and frequent mitosis in the focal area of the tumor, characteristics suggestive of the cellular variant of CMN. Heterogeneous mesenchymal elements, such as cartilage and fat, were also noted. The final pathological diagnosis was mixed CMN with focal cellular variant (less than 10%).

At seven weeks of age, local tumor recurrence was detected in the left retroperitoneum on abdominal US. It was observed as a complex cystic mass similar to the primary mass. This local tumor recurrence grew rapidly during the follow-up period. Its longest diameter increased from 5 cm to 8.6 cm in just two weeks. At nine weeks of age, a whole body MRI with DWI showed a recurrent cystic mass in the left retroperitoneum with one newly developed hepatic nodular lesion (Fig. 1F-I). The lesion in the liver

showed low signal intensity on the T1-weighted images and high signal intensity on the T2-weighted images. In addition, this hepatic lesion showed diffusion restriction on DWI, although the recurrent lesion did not. The ADC value of the liver lesion was  $1.99 \times 10^{-3} \text{ mm}^2/\text{sec}$  and the ADC value of the surrounding liver parenchyma was  $2.37 \times 10^{-3} \text{ mm}^2/\text{sec}$ . A chest CT showed no visible metastatic lesions. The patient responded well to a chemotherapy regimen composed of vincristine, dactinomycin, and endoxan. After four months, no tumor was grossly found remaining in both the retroperitoneum and liver on MRI; this finding was also supported by no visible tumor on the operation field, which was performed for intestinal obstruction secondary to adhesions. Therefore, the hepatic nodular lesion was considered as metastasis. So far, during a 7 month follow-up period after the detection of local tumor recurrence, the patient has undergone 8 cycles of chemotherapy without evidence of tumor growth.

## DISCUSSION

Congenital mesoblastic nephroma, a hamartomatous renal tumor composed predominantly of spindle cells and

fibroblasts, is the most common renal mass observed in infants less than three months old (2). Other differential diagnoses of perinatal renal or retroperitoneal tumors include Wilms' tumor, nephroblastomatosis, multilocular cystic renal tumor, clear cell sarcoma, rhabdoid tumor, ossifying renal tumor of infancy, and teratoma (11).

Generally, CMN is a solid lesion found either localized within or more commonly extending from the renal parenchyma. The lesion may extend to the renal vessels or the inferior vena cava, but does not invade them (12). It has two pathological subtypes of the classic variant and the cellular variant. Further, these subtypes show different imaging findings and clinical characters. US of the classic variant reveals a solid or predominantly solid tumor with a hypochoic ring. The cellular variant, on the other hand, shows characteristics of intratumoral hemorrhage and cystic or necrotic portions (5). The cellular variant also commonly shows perirenal invasion and local recurrence (3). In our case, the mass appeared mainly cystic, which is a character of cellular variant, although the pathologic result revealed mainly classic variant with a small portion of cellular variant.

Other studies with CT images have shown a large, uniform soft tissue mass with minimal peripheral enhancement for CMN. Focal enhancement, necrosis, and hemorrhage have been reported as characteristics of the cellular variant in these studies. In comparison to CT studies, fetal MRI findings have been variable and inconsistent with isolated reports in published literature, as few cases of CMN are evaluated with MRI. However, CMN has been described as having low or intermediate signal intensity on T1-weighted images before and after gadolinium administration (5). Similarly on T2-weighted images, the mass has been described as having markedly low to predominantly high signal intensity in comparison to the surrounding renal parenchyma (7). Our case also showed low signal intensity on T1-weighted images and intermediate signal intensity on T2-weighted images of the solid portions of the tumor.

Diffusion-weighted imaging showed true diffusion restriction in the solid portions of the mass in our case. There have been many studies using DWI in tumor evaluation, but little is known of its use in evaluating pediatric renal tumors. Humphries et al. (8) studied DWI in pediatric extracranial masses, including five renal tumors of three nephroblastomas, one rhabdoid tumor and one multilocular cystic nephroma. In addition, they concluded that there was an inverse relationship between ADC and

cellularity. However, ADC could not differentiate between benign and malignant tumors. Zhang et al. (9) reported the difference of ADCs in renal lesions of benign cyst, necrotic or cystic portion, and solid enhancing portion of tumor. However, the T1 signal was related to the ADC of the lesion. Taouli et al. (10) reported that DWI is useful in the differential diagnosis between the subtypes of renal cell carcinoma. They said that restricted diffusion in renal tumors can be multifactorial with relations to tissue cellularity, degree of cell membrane integrity, and the combined effects of capillary perfusion and diffusion. However, there have been no reports of DWI findings of CMN. Our case showed diffusion restriction in the solid portion of the primary mass on DWI, and this may be related to the increased cellularity of this portion. During follow up, early tumor recurrence was found with rapid growth. However, a follow up whole body MRI undergone to evaluate possible metastasis showed the recurrent mass as a cystic lesion with no diffusion restriction. In contrast, the hepatic lesion showed signal characteristics similar to that of the solid portions of the primary mass, including diffusion restriction on DWI. Although most CMNs have a favorable outcome, our case showed early local recurrence and suspicious metastasis. Further study is required to determine the relationship between the diffusion restriction on DWI, pathological features, and prognosis of CMN.

This case is significant in being the first report of DWI finding of CMN on prenatal and postnatal MRI. The primary mass was huge and mainly cystic with solid portions that showed diffusion restriction on prenatal MRI, which may be related to the increased cellularity of cellular variant portion on pathology. Early local tumor recurrence and suspicious liver metastasis were detected on postnatal MRI with diffusion restriction also being observed in the hepatic lesion. In conclusion, our case demonstrates that CMN with cellular variant can show diffusion restriction on DWI. We reflect that further evaluation of restricted diffusion and its significance and possible association with the pathological features and disease prognosis of CMN is needed.

## REFERENCES

1. Bolande RP, Brough AJ, Izant RJ Jr. Congenital mesoblastic nephroma of infancy. A report of eight cases and the relationship to Wilms' tumor. *Pediatrics* 1967;40:272-278
2. Powis M. Neonatal renal tumours. *Early Hum Dev* 2010;86:607-612
3. Joshi VV, Kay S, Milsten R, Koontz WW, McWilliams NB.

- Congenital mesoblastic nephroma of infancy: report of a case with unusual clinical behavior. *Am J Clin Pathol* 1973;60:811-816
4. Bayindir P, Guillerman RP, Hicks MJ, Chintagumpala MM. Cellular mesoblastic nephroma (infantile renal fibrosarcoma): institutional review of the clinical, diagnostic imaging, and pathologic features of a distinctive neoplasm of infancy. *Pediatr Radiol* 2009;39:1066-1074
  5. Chaudry G, Perez-Atayde AR, Ngan BY, Gundogan M, Daneman A. Imaging of congenital mesoblastic nephroma with pathological correlation. *Pediatr Radiol* 2009;39:1080-1086
  6. Chan HS, Cheng MY, Mancer K, Payton D, Weitzman SS, Kotecha P, et al. Congenital mesoblastic nephroma: a clinicoradiologic study of 17 cases representing the pathologic spectrum of the disease. *J Pediatr* 1987;111:64-70
  7. Puvaneswary M, Roy GT. Congenital mesoblastic nephroma: other magnetic resonance imaging findings. *Australas Radiol* 1999;43:532-534
  8. Humphries PD, Sebire NJ, Siegel MJ, Olsen ØE. Tumors in pediatric patients at diffusion-weighted MR imaging: apparent diffusion coefficient and tumor cellularity. *Radiology* 2007;245:848-854
  9. Zhang J, Tehrani YM, Wang L, Ishill NM, Schwartz LH, Hricak H. Renal masses: characterization with diffusion-weighted MR imaging--a preliminary experience. *Radiology* 2008;247:458-464
  10. Taouli B, Thakur RK, Mannelli L, Babb JS, Kim S, Hecht EM, et al. Renal lesions: characterization with diffusion-weighted imaging versus contrast-enhanced MR imaging. *Radiology* 2009;251:398-407
  11. Lowe LH, Isuani BH, Heller RM, Stein SM, Johnson JE, Navarro OM, et al. Pediatric renal masses: Wilms tumor and beyond. *Radiographics* 2000;20:1585-1603
  12. Riccabona M. Imaging of renal tumours in infancy and childhood. *Eur Radiol* 2003;13 Suppl 4:L116-L129